Supplementary File

Complementary Early-Phase Magnetic Particle Imaging and Late-Phase Positron Emission Tomography Reporter Imaging of Mesenchymal Stem Cells In Vivo

Shalaby, Nourhan[1]
Kelly, John J.[2]
Sehl, Olivia C.[1]
Gevaert, Julia J.[1]
Fox, Matthew S.[3,4]
Qi, Qi[2,3,5]
Foster, Paula J.[2]
Thiessen, Jonathan D.[2,4]
Hicks, Justin W.[1,3]
Scholl, Timothy J.[1,2,5]
Ronald, John A.[1,2,3,7]

[1] Department of Medical Biophysics, Schulich School of Medicine and Dentistry, Western University, London, ON
[2] Robarts Research Institute, Schulich School of Medicine and Dentistry, Western University, London, ON
[3] Lawson Health Research Institute, London, ON
[4] Saint Joseph's Health Care, London, ON
[5]Ontario Institute for Cancer Research, Toronto, ON
[6] Department of Microbiology & Immunology, Schulich School of Medicine and Dentistry, Western University, London, ON

Corresponding Author: John Ronald; jronald@robarts.ca; 519-931-5777 x24391

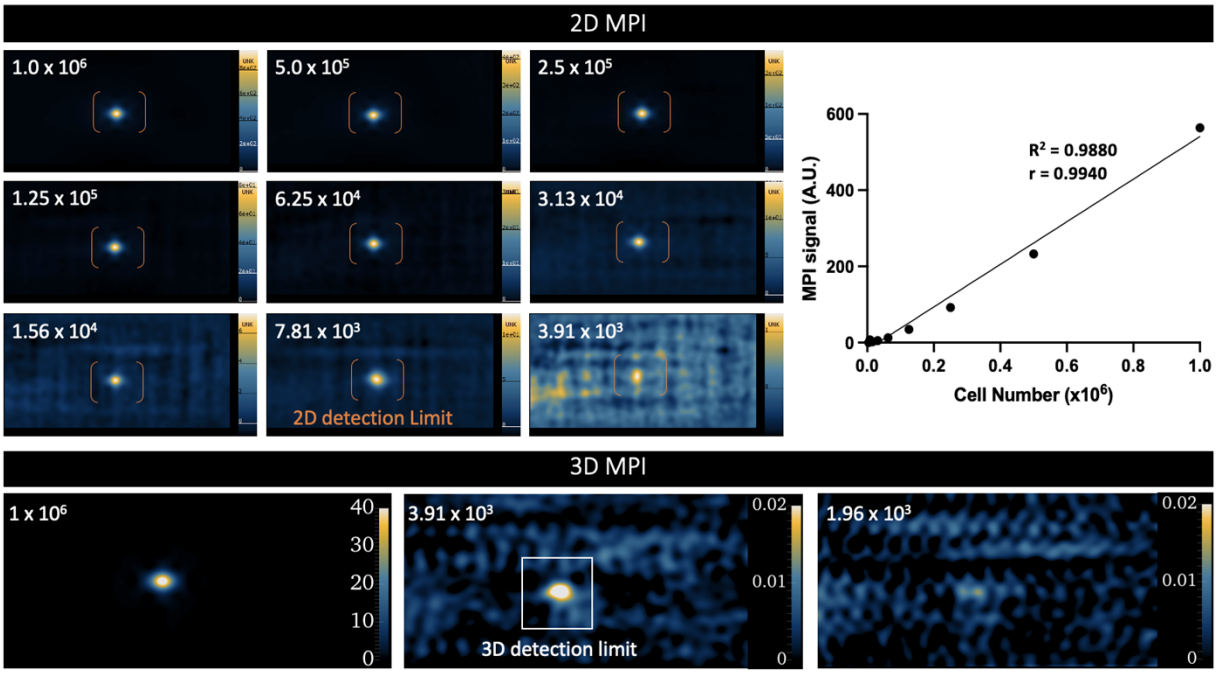

Figure 1: **Calibration images for MPI quantification and detection threshold estimation of Synomag-D-labelled cells.** In-vitro MPI detection of various numbers of Synomag-D-labelled MSCs (ranging from 10^6-<4,000 cells), showing a 2D cellular detection limit of <8,000 cells, and a 3D detection limit of <4,000 cells. MPI signal was shown to strongly correlate with cell number (R^2=0.9880).

Supplementary Figures 2 and 3 below show the in-vivo tracking of the tri-modally detectable MSCs in two additional mice. In-vivo detection of MSCs in the hind limb with MPI (top), BLI (middle) and PET (bottom) in each mouse over a 30-day period. MPI shows the brightest signal on day 0 and steadily decreases over time. BLI signal shows fluctuating radiance (initial signal reduction due to cell death), followed by an ultimate increase in BLI signal thereafter. PET SUV shows a similar pattern to BLI radiance at the comparable imaging timepoints of the engineered MSCs (arrows). Additional uptake also present in thyroid and stomach (organs with endogenous NIS expression).

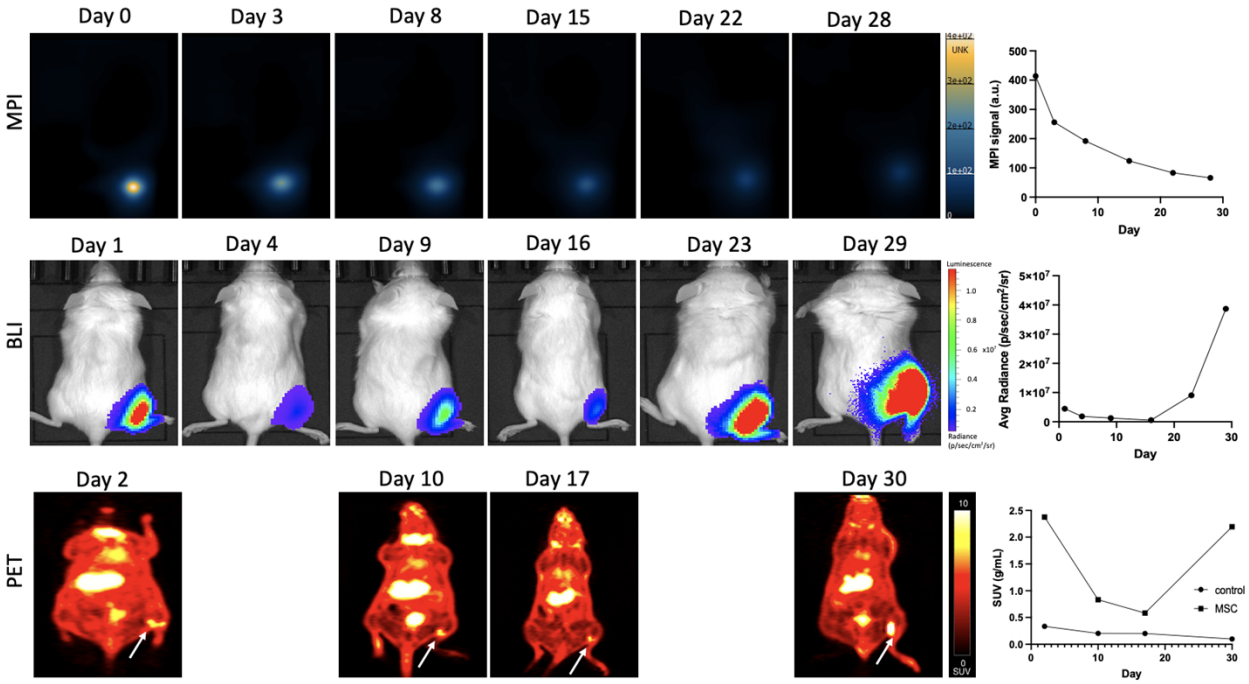

Supplementary Figure 2: Mouse Identifier: Mouse 1

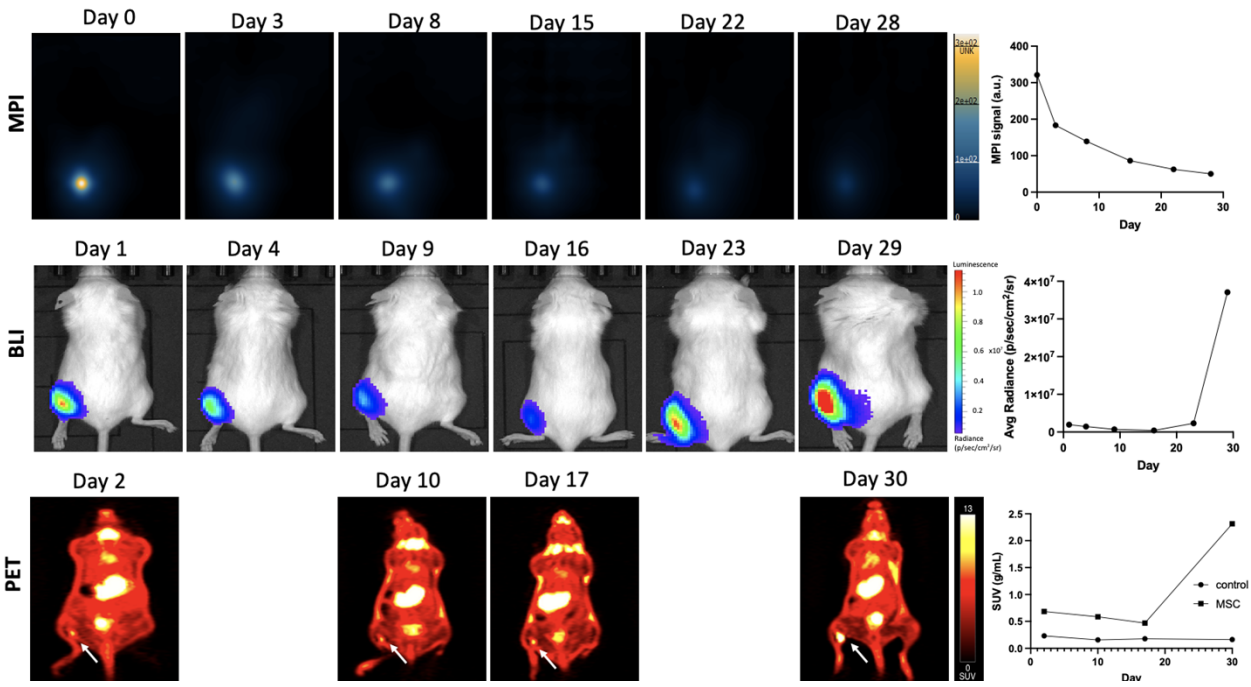

Supplementary Figure 3: Mouse Identifier: Mouse 2

Supplementary Figures 4 and 5 below show the in-vivo tracking of the MSCs in the remaining two mice. Imaging MSCs with MPI (top), BLI (middle) and PET (bottom) was performed. Similar to previous mice, MPI signal showed bright signal on day 0 that steadily decreased over time. BLI signal also allowed the detection of MSCs and showed fluctuating patterns but with overall lower radiance (on the order of 10^6 p/sec/cm2/sr for all imaging time points in comparison to the previous mice. This decrease in MSC signal can be mainly attributed to eventual cell death and clearance. Mice represented in figures 4 and 5 did not display detectable MSC PET signal.

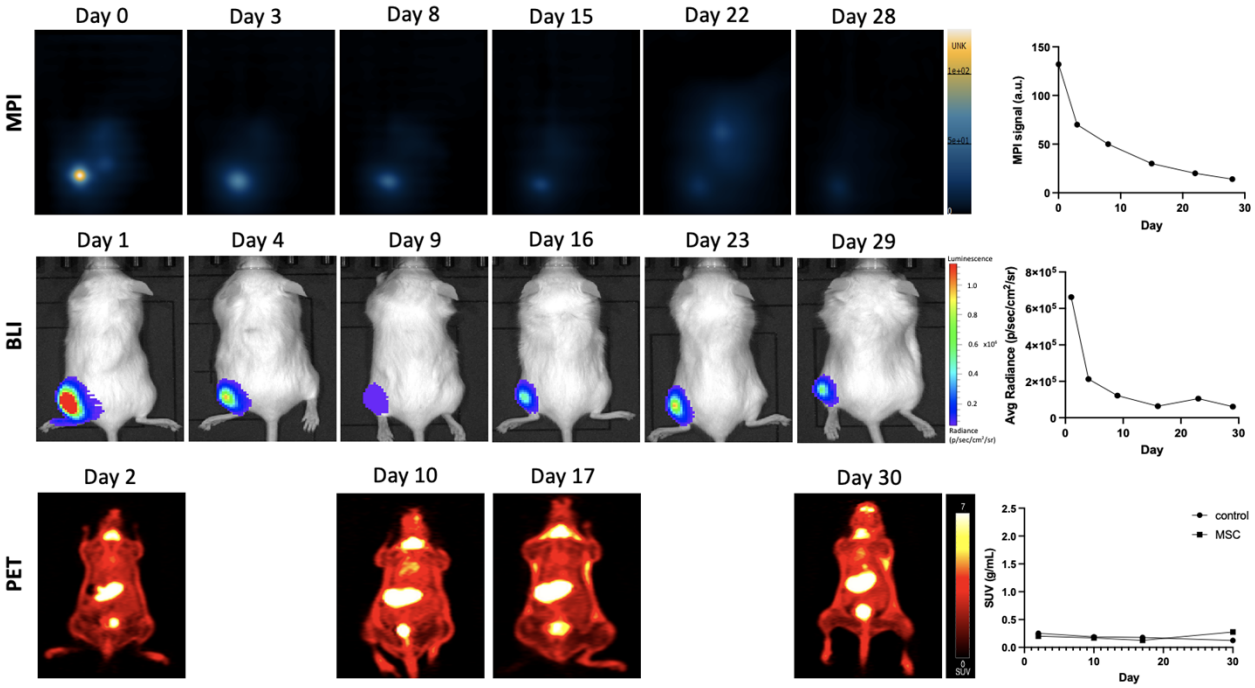

Supplementary Figure 4: Mouse Identifier: Mouse 3

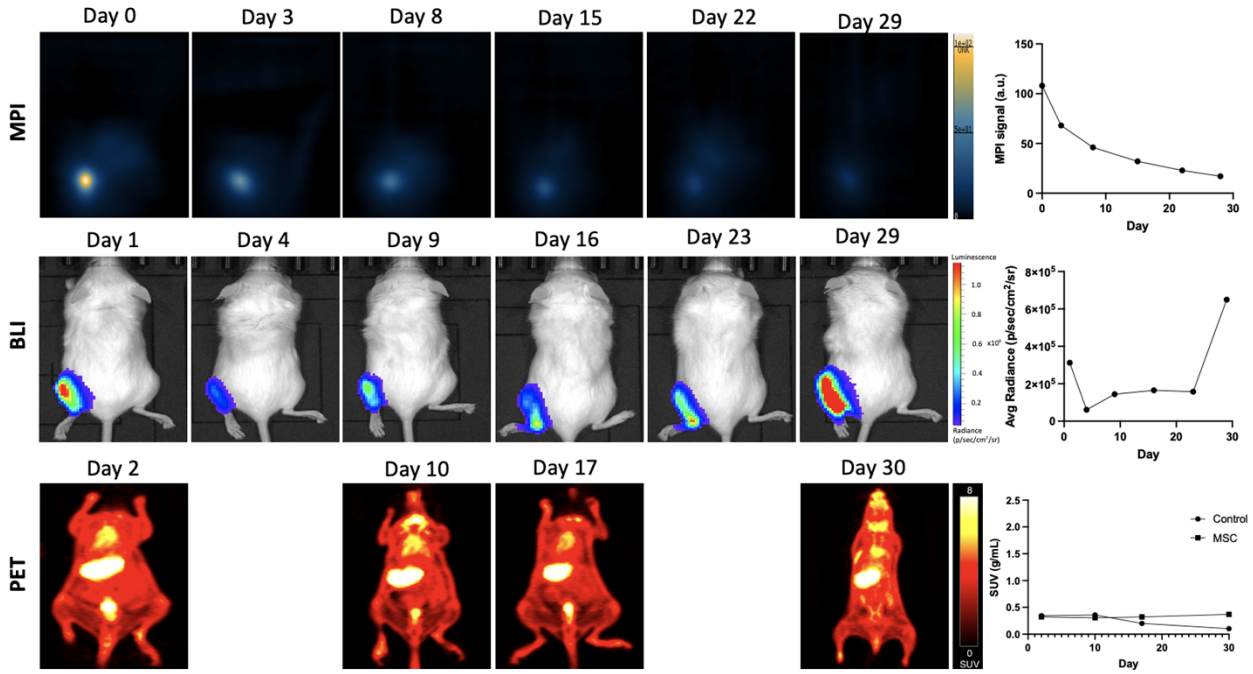

Supplementary Figure 5: Mouse Identifier: Mouse 5

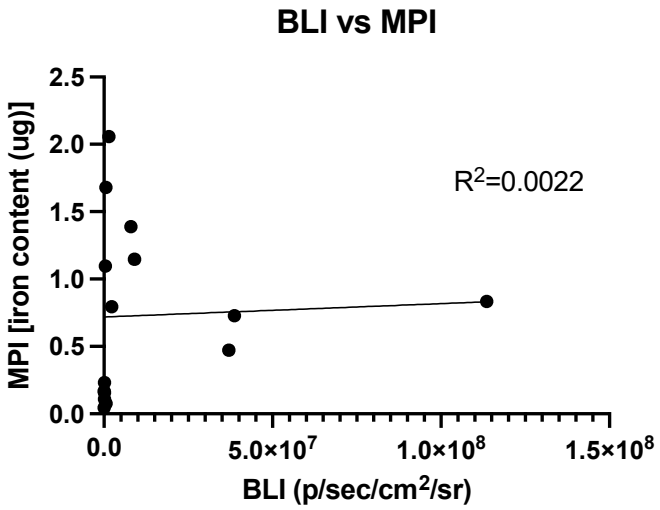

Supplementary Figure 6: Correlation plot between BLI signal and MPI signal at later imaging time points (day 10-30). Plot showing weak correlation between MPI signal and BLI radiance at late phase imaging (R^2=0.0022).